

Electronic Structure Description of the μ_4 -Sulfide Bridged Tetranuclear Cu_2 Center in N_2O ReductasePeng Chen,[†] Serena DeBeer George,[†] Inês Cabrito,[‡] William E. Antholine,[§] José J. G. Moura,[‡] Isabel Moura,^{*,‡} Britt Hedman,^{†,||} Keith O. Hodgson,^{†,||} and Edward I. Solomon^{*,†}

Department of Chemistry, Stanford University, Stanford, California 94305, Departamento de Química, CQFB, Faculdade de Ciências e Tecnologia, Universidade Nova de Lisboa, 2825-114 Caparica, Portugal, Biophysics Research Institute, Medical College of Wisconsin, Milwaukee, Wisconsin 53226, Stanford Synchrotron Radiation Laboratory, SLAC, Stanford University, Stanford, California 94309

Received August 29, 2001

Nitrous oxide reductase (N_2OR) catalyzes the two-electron reduction of the green house gas N_2O (produced by denitrification and other processes) to N_2 and H_2O in the terminal step of anaerobic metabolism and is involved in ATP synthesis.¹ The crystal structures of N_2OR from *Pseudomonas nautica* (Pn) and *Paracoccus denitrificans* (Pd) were recently solved.^{2,3} The dimeric protein contains a Cu_A center and a Cu_Z center in each subunit. The Cu_Z center has a μ_4 -sulfide bridged tetranuclear Cu cluster with seven His ligands and a water-derived ligand (the water position is uncertain in the Pn crystal structure, vide infra), and shows unusual electronic^{4,5} and vibrational⁶ spectral features. The purpose of this study is to use a combination of saturation magnetic circular dichroism (MCD), Cu K-edge X-ray absorption spectroscopy (XAS), multifrequency EPR, and density functional theory (DFT) calculations to determine the spin state, oxidation states, electron spin distribution, and the ground-state wave function of the Cu_Z center in the dithionite reduced form of N_2OR from Pn where the Cu_A center is completely reduced,⁷ and to correlate the ground-state wave function to reactivity.

Variable-temperature, variable-field saturation (VTVH) MCD was used to determine the spin state of the Cu_Z center, where the MCD intensity of different possible spin states will show different saturation behavior.⁸ Figure 1 inset shows the 5 K 7 T MCD spectrum of Cu_Z , similar to that reported in the literature.⁵ The saturation data of the Cu_Z MCD intensity at 620 nm at various temperatures are plotted along with simulated saturation curves for $S = 1/2$, 1, and $3/2$ systems assuming isotropic polarization and g values (Figure 1). The data clearly indicate that the Cu_Z center has an $S_{\text{Total}} = 1/2$ ground state.^{9,10}

With four Cu atoms having an $S_{\text{Total}} = 1/2$, the Cu_Z center oxidation state can be one Cu^{II} and three Cu^{I} , or three Cu^{II} and one Cu^{I} . Cu K-edge XAS was used to distinguish between these possibilities, where Cu^{I} complexes have a characteristic feature at ~ 8984 eV while Cu^{II} complexes have no peak maximum below 8985 eV (except for a weak $\text{Cu } 1s \rightarrow 3d$ transition at 8979 eV).¹¹ The Cu K-edge spectrum of the Cu_Z center is shown in Figure 2.¹² The data were simulated with use of Cu^{II} to Cu^{I} ratios of 3:1 and 1:3 (Figure 2).¹³ The simulations clearly show that the $1\text{Cu}^{\text{II}}/3\text{Cu}^{\text{I}}$ model is far better than the $3\text{Cu}^{\text{II}}/1\text{Cu}^{\text{I}}$ alternative, thus indicating that there is only one oxidized Cu in the Cu_Z center and that the Cu oxidation states are $1\text{Cu}^{\text{II}}/3\text{Cu}^{\text{I}}$.¹⁴

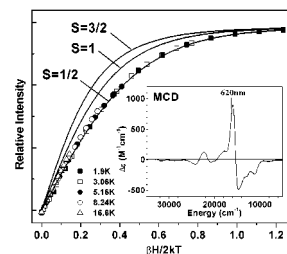


Figure 1. Saturation MCD (points) of Cu_Z along with simulated saturation curves (solid lines). Inset: 5 K 7 T MCD spectrum of Cu_Z .

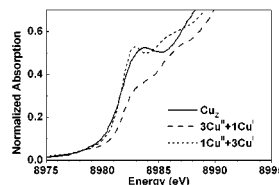


Figure 2. Cu K-edge XAS spectrum of Cu_Z and simulated spectra assuming $3\text{Cu}^{\text{II}} + 1\text{Cu}^{\text{I}}$ and $1\text{Cu}^{\text{II}} + 3\text{Cu}^{\text{I}}$.

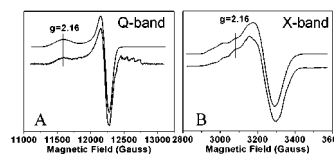


Figure 3. Experimental (lower) and simulated (upper) EPR spectra of Cu_Z : (A) Q-band, 35.001 GHz, 15 K; (B) X-band, 9.319 GHz, 77 K.

EPR spectroscopy was used to determine the unpaired electron spin distribution (i.e. of one Cu^{II}) of this Cu_Z center. The X-band EPR spectrum of Cu_Z has been reported⁴ and shows metal hyperfine structure in the g_{II} region (Figure 3B, lower). The analysis of the hyperfine coupling is not clear due to the broad signal. Consequently the system g values could not be accurately determined. Therefore Q-band EPR was used to map the system g values. The EPR spectrum of Cu_Z at Q-band (Figure 3A, lower) is very close to that of an axial system with $g_{\text{II}} \approx 2.16 > g_{\perp} \approx 2.04 > 2.0$, indicating that the metal 3d electron hole resides in a $\text{Cu } d_{x^2-y^2}$ orbital.^{15,16} Given these g values, simultaneous fitting of the EPR spectra at Q- and X-band requires at least a second Cu to account for the metal hyperfine pattern observed at X-band (Figure 3A,B, upper), with one Cu center dominating the hyperfine splitting ($A_{\text{II}} = 61 \times 10^{-4} \text{ cm}^{-1}$) and a second Cu contributing another $\sim 30\%$ of the spin ($A_{\text{II}} = 24 \times 10^{-4} \text{ cm}^{-1}$).^{17,18} Thus the single electron spin of the Cu_Z center partially delocalizes over at least two Cu centers with a $\sim 5:2$ spin distribution. The ground state is a class II partially

* To whom correspondence should be addressed.

[†] Department of Chemistry, Stanford University.

[‡] Universidade Nova de Lisboa.

[§] Wisconsin Medical College.

^{||} Stanford Synchrotron Radiation Laboratory.

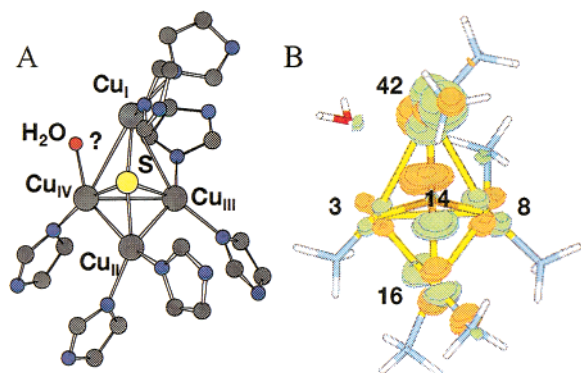


Figure 4. (A) Crystal structure of the Cu_2 center of N_2OR from Pn. (B) DFT calculated lowest unoccupied spin-down molecular orbital. Spin distributions (%) are labeled on the Cu and S atoms. Contours are drawn at $\pm 0.05, 0.10, 0.15, 0.20$ [e/bohr^3] $^{1/2}$.

delocalized mixed-valent system¹⁹ with the single 3d electron hole dominantly in a $d_{x^2-y^2}$ orbital on one Cu center.

The crystal structure (Figure 4A),^{20,21} spin state ($S = 1/2$), and Cu oxidation states ($1\text{Cu}^{\text{II}}/3\text{Cu}^{\text{I}}$) were input into a spin-unrestricted DFT calculation to obtain a description of the ground-state wave function of the Cu_2 center.²² The histidine ligands were modeled as NH_3 . Hybrid DFT calculations have been widely used in the study of Cu sites in proteins. The calculations are found to be very sensitive to the amount of Hartree–Fock exchange included in the hybrid functional. A spectroscopically calibrated hybrid functional is used here (38% Hartree–Fock exchange added to the BP86 functional).²³ Figure 4B gives the lowest unoccupied spin down molecular orbital of the Cu_2 center, which is equivalent to the singly occupied molecular orbital in a spin-restricted formalism and reflects the ground state wave function and its spin distribution. The calculated wave function is partially delocalized and the Cu_I is the dominantly oxidized copper center (42%) while Cu_II is the second Cu, which has significant spin density (16%). The spin distribution has a $\sim 5:2$ ratio on these two Cu's, consistent with the Q-/X-band EPR results. There is also some spin delocalization over Cu_III (8%) and Cu_IV (3%). The μ_4 -bridging sulfide also has significant contribution to the ground-state wave function (14%) and forms a dominant σ -bonding interaction ($\text{Cu}_\text{I}\text{--S--Cu}_\text{II}$ angle $\approx 165^\circ$) with the $d_{x^2-y^2}$ orbitals of Cu_I and Cu_II ,²⁴ which constitutes an excellent σ superexchange pathway between Cu_I and Cu_II for electron delocalization.

In summary, the μ_4 -sulfide bridged tetranuclear Cu_2 center is an $S_{\text{Total}} = 1/2$ system with one oxidized Cu and the spin mainly residing on Cu_I with significant contribution from Cu_II and the approximately linear bridging sulfide.²⁵ This ground-state wave function of Cu_2 provides initial possible insight into the enzymatic reactivity of N_2O reduction. The substrate binding edge² (involving both Cu_I and Cu_IV) of Cu_2 has one dominantly oxidized Cu_I and one dominantly reduced Cu_IV center. This should favor the N_2O interaction (possibly bridging) and oxo transfer, while providing the capability for overcoming the reaction barrier²⁶ by simultaneous two-electron reduction of N_2O . One electron can be donated directly from Cu_IV and the other from Cu_II through the $\text{Cu}_\text{II}\text{--S--Cu}_\text{I}$ σ superexchange pathway. Additionally, the Cu_IV and Cu_II centers have good electron-transfer pathways from the two bridging thiolates of the neighboring Cu_A center in the dimeric protein, allowing rapid rereduction in turnover.^{27,28}

Acknowledgment. This research is supported by NIH DK-31450 (E.I.S.), RR-01209 (K.O.H.), and PRAXIS (J.J.G.M. and I.M.). SSRL operations are funded by DOE, BES. The Structural

Molecular Biology program is supported by NIH, NCRR, BTP and by DOE, BER. P.C. is a Gerhard Casper Stanford Graduate Fellow. I.C. has a PRAXIS-BD fellowship.

Supporting Information Available: Coordinates for Cu_2 model calculation and additional simulation of Cu_2 K-edge (PDF). This material is available free of charge via the Internet at <http://pubs.acs.org>.

References

- (1) Zumft, W. G. *Microbiol. Mol. Biol. Rev.* **1997**, *61*, 533.
- (2) Brown, K.; Tegoni, M.; Prudencio, M.; Pereira, A. S.; Besson, S.; Moura, J. J.; Moura, I.; Cambillau, C. *Nat. Struct. Biol.* **2000**, *7*, 191.
- (3) Brown, K.; Djinnovic-Carugo, K.; Haltia, T.; Cabrito, I.; Saraste, M.; Moura, J. J. G.; Moura, I.; Tegoni, M.; Cambillau, C. *J. Biol. Chem.* **2000**, *275*, 41133.
- (4) Prudencio, M.; Pereira, A. S.; Tavares, P.; Besson, S.; Cabrito, I.; Brown, K.; Samyn, B.; Devreese, B.; VanBeeumen, J.; Rusnak, F.; Fauque, G.; Moura, J. J. G.; Tegoni, M.; Cambillau, C.; Moura, I. *Biochemistry* **2000**, *39*, 3899.
- (5) Rasmussen, T.; Berks, B. C.; Sanders-Loehr, J.; Dooley, D. M.; Zumft, W. G.; Thomson, A. J. *Biochemistry* **2000**, *39*, 12753.
- (6) Alvarez, M. L.; Ai, J. Y.; Zumft, W.; Sanders-Loehr, J.; Dooley, D. M. *J. Am. Chem. Soc.* **2001**, *123*, 576.
- (7) The N_2OR sample was isolated and purified as in ref 4. The Cu_2 sample was prepared by adding excess dithionite solution to the N_2OR protein sample in deuterated Tris/DCI buffer, pH 7.3. 60% glycerol- d_3 was added for the MCD measurement as glassing agent.
- (8) Neese, F.; Solomon, E. I. *Inorg. Chem.* **1999**, *38*, 1847.
- (9) This is consistent with spin quantitation results. See ref 4.
- (10) Farrar, J. A.; Thomson, A. J.; Cheesman, M. R.; Dooley, D. M.; Zumft, W. G. *FEBS Lett.* **1991**, *294*, 11.
- (11) Kau, L. S.; Spira-Solomon, D. J.; Penner-Hahn, J. E.; Hodgson, K. O.; Solomon, E. I. *J. Am. Chem. Soc.* **1987**, *109*, 6433.
- (12) Cu K-edge data were obtained as described in: DeBeer, S.; Randall, D. W.; Nersissian, A. M.; Valentine, J. S.; Hedman, B.; Hodgson, K. O.; Solomon, E. I. *J. Phys. Chem.* **2000**, *104*, 10814. The Cu K-edge of Cu_2 was obtained by subtracting the edge of fully reduced Cu_A (from the soluble domain of cytochrome oxidase from *T. thermophilus*) from that of the dithionite reduced N_2OR and renormalized to an edge jump of 1.
- (13) The Cu K-edge data were modeled with use of Cu^{I} and Cu^{II} complexes with an average 3-coordinate environment, consisting of 2 nitrogens and 1 sulfur ligation. A reasonable fit to the data requires models with sulfur ligation.
- (14) Simulations where the edge was shifted to account for the different average oxidation states (i.e. an average state of 1.25 or 1.75) were also performed. The results clearly favor an average oxidation state of 1.25 and hence only one Cu^{II} (Figure S1).
- (15) Solomon, E. I. *Comments Inorg. Chem.* **1984**, *3*, 227.
- (16) The high field features in the Q-band spectrum are due to manganese contamination in the cavity.
- (17) An EPR simulation program developed by Frank Neese was used (Neese, F.; Zumft, W. G.; Antholine, W. E.; Kroneck, P. M. H. *J. Am. Chem. Soc.* **1996**, *118*, 8692.). The spin Hamiltonian eigenvalues are solved to first order in perturbation theory. Parameters used in the simulation follow: $g_x = g_y = 2.043$, $g_z = 2.160$, $A_x = 61 \times 10^{-4} \text{ cm}^{-1}$, $A_z = 24.4 \times 10^{-4} \text{ cm}^{-1}$. Hyperfines of A_x and A_y are not resolved and the perpendicular region was simply simulated with a g value and line widths. Bandwidth: X-band, $W_x = W_y = 54 \text{ G}$, $W_z = 24 \text{ G}$; Q-band, $W_x = W_y = 65 \text{ G}$, $W_z = 112 \text{ G}$.
- (18) This is also consistent with S-band EPR results. Chen, P.; Antholine, W. E.; Solomon, E. I. Unpublished results.
- (19) Robin, M. B.; Day, P. *Adv. Inorg. Radiochem.* **1967**, *10*, 247.
- (20) The structural parameters were taken from the crystal structure of N_2OR from Pn and averaged over two monomers. M–M and M–L bonds are adjusted to the more accurate values of the Pd N_2OR structure. The calculations are relatively insensitive to these structural modifications.
- (21) The absorption spectrum of the Pn N_2OR crystal indicates that the oxidation state of Cu_2 in the structure in Figure 4A is the same as that in the dithionite reduced form of N_2OR studied here. See ref 2.
- (22) The computational package Gaussian98 was used for the DFT calculations.
- (23) Szilagyi, R.; Metz, M.; Solomon, E. I. *J. Phys. Chem. A*, in press.
- (24) For the local coordinate systems on each Cu center, the x -axis is set along the Cu–S bond and the z -axis is perpendicular to the d orbital plane in Figure 4B.
- (25) Recent CW-ENDOR results are consistent with the ground-state wave function described here. Brondino, C. D.; Doan, P. E.; Cabrito, I.; Besson, S.; Moura, J. J. G.; Moura, I.; Hoffman, B. M. To be submitted for publication.
- (26) Jolly, W. L. *The Inorganic Chemistry of Nitrogen*; W. A. Benjamin: New York, 1964.
- (27) George, S. D.; Solomon, E. I. Unpublished results.
- (28) George, S. D.; Metz, M.; Szilagyi, R. K.; Wang, H.; Cramer, S. P.; Lu, Y.; Tolman, W. B.; Hedman, B.; Hodgson, K. O.; Solomon, E. I. *J. Am. Chem. Soc.* **2001**, *123*, 5757.

JA0169623